Available online at www.sciencedirect.com
SCIENCE DIRECT
Polymer 46 (2005) 7855–7866
polymer
www.elsevier.com/locate/polymer

Polypropylene–polyhedral oligomeric silsesquioxanes (POSS) nanocomposites

Alberto Fina, Daniela Tabuani*, Alberto Frache, Giovanni Camino

Centro di Cultura per l'Ingegneria delle Materie Plastiche, Politecnico di Torino, V.le Michel 5, 15100 Alessandria, Italy

Received 7 April 2005; received in revised form 22 June 2005; accepted 30 June 2005

Abstract

In this paper, the influence of the functionalisation of polyhedral oligomeric silsesquioxanes (POSS) cages on the preparation and properties of polypropylene (PP) based nanocomposites is studied.

POSS with different chain lengths (octamethyl-, octaisobutyl- and octaisooctyl-POSS) are taken in to account and melt mixed with PP. The resulting composites are characterised as regards thermal and morphological characteristics by means of DSC, TGA, SEM and X-ray diffraction.

A good dispersion is obtained particularly at low loadings of POSS functionalised with longer organic chains.

Important features are recognised as regards the crystallisation behaviour of PP by octamethyl- and octaisobutyl-POSS: The former acting as a nucleating agent and the second inducing PP polymorphism.

Keywords: POSS; Nanocomposites; Thermal behaviour

1. Introduction

In the past decade, researchers' interest has been widely attracted by the possibility to prepare hybrids and nanocomposites starting from inorganic cage molecules constituted by a silicon–oxygen based framework.

These molecules, named polyhedral oligomeric silsesquioxanes (POSS), firstly synthesised in 1946 [1], belong to the wide family of silsesquioxanes, characterised by the general formula $(RSiO_{1,5})_n$ where R is hydrogen or an organic group, such as alkyl, aryl or any of their derivatives.

POSS molecules are physically large with respect to monomer dimensions and nearly equivalent in size to most polymer segments.

POSS are usually produced by hydrolytic condensation of trifunctional monomers $RSiX_3$, where X is a highly reactive substituent, such as Cl or alkoxy [2,3].

Neat POSS are used as low dielectric constant materials, new resists for electron beam lithography materials, high temperature lubricants or catalysts [4,5].

Even though the first synthesis of these structures can be traced back in the 1950s, only in the past 10 years POSS have attracted wide-spread interest mainly as precursors to hybrid inorganic/organic materials [6].

In this regard, POSS are surely attractive materials as they can be easily functionalised by chemically altering the R substituent groups, thus having the potentiality of undergoing copolymerisation or grafting reactions. Several polymeric systems have been taken in to account incorporating POSS cages both in thermoplastic matrices, such as styryl-based polymers [7–9], acrilates [10–13], olefines [14–17], and in thermosets, mainly as regards epoxy resins [18–21].

From a general point of view, the presence of the thermally robust POSS moiety was found to drastically modify the polymer thermal properties supplying greater thermal stability to the polymer matrix, also allowing the tailoring of the polymer glass transition temperature by tuning the POSS concentration.

Moreover, incorporation of POSS molecules was responsible for improvements of the mechanical properties

* Corresponding author. Address: Centro di Cultura per l'Ingegneria delle Materie Plastiche, Politecnico di Torino, V.le Michel 5, 15100 Alessandria, Italy. Tel.: +39 131229361; fax: +39 131229331.
E-mail address: daniela.tabuani@polial.polito.it (D. Tabuani).

0032-3861/$ - see front matter © 2005 Elsevier Ltd. All rights reserved.
doi:10.1016/j.polymer.2005.06.121

as well as reductions in flammability and heat evolution in combustion [16].

Very few works have been reported so far as regards the preparation of nanocomposites with non-reactive POSS. One of these papers studies the incorporation of phenyl-trisilanol POSS in epoxy–amine networks and the influence of the inorganic concentration on the thermo-mechanical properties of the final composites [22].

As far as polyolefins are concerned, the possibility to fine tuning POSS cage interfacial properties, by playing on the substituent group nature is even more appealing, as it was reported that in polyolefins–clay systems the formation of nanocomposites (either intercalated or exfoliated) is impeded by the unfavourable interactions between hydrophilic clay surfaces and hydrophobic polyolefins [23]. Even by using chemically modified organphilic clays and a compatibiliser such as maleic anhydride grafted polyolefin, it is difficult to obtain an exfoliated structure [24].

Fu et al. [25] reported the first study concerning PP/POSS composites evaluating their crystallisation behaviour, at quiescent and shear states. Octamethyl-POSS was added by melt blending in an internal mixer to *i*-PP at quite large concentrations (10, 20 and 30 wt%) and the crystallisation behaviour was studied by means of DSC and in situ SAXS measurements. POSS was found to influence quiescent melt crystallisation enhancing (by acting as a nucleating agent) or retarding the crystallisation process, depending on its concentration. Whereas, under shear, the POSS always accelerated such mechanism.

More recently, the same research group investigated the physical gelation in ethylene–propylene (EP) copolymer melts induced by POSS molecules [26]. EP/octamethyl–POSS composites were prepared by melt-mixing in a twin-screw microcompounder with EP copolymers characterised by different ethylene contents and varying the POSS loadings from 10 to 30 wt%.

From WAXD analysis it was found that no molecular dispersion of POSS cages could be achieved as POSS X-ray pattern was maintained in the composites. Small-amplitude oscillatory shear experiments showed that the presence of POSS molecules changed the rheological behaviour above melting from liquid-like in the neat resin to solid-like in the nanocomposites. Moreover, the addition of 10 wt% of POSS was found to increase considerably the Young's modulus and the T_g value (both calculated by means of DMA analysis) as compared to neat EP.

The nonisothermal crystallisation of HDPE/POSS nanocomposites was very recently studied by Joshi et al. [27]: The crystallinity of HDPE was found to be dependent on the amount of added octamethyl-POSS and on the cooling rates.

In this paper, we present an extensive study to evaluate the influence of the POSS substituent groups on the morphological and thermal characteristics of melt-blended POSS/PP composites. In particular the influence of the aliphatic chain length is studied by preparing composites with octamethyl-, octaisobutyl- and octaisooctyl-POSS.

2. Materials and methods

Octamethyl-, octaisobutyl- and octaisooctyl-POSS (from now on referred to as ome-, oib-, and oic-POSS, respectively) were used as purchased from Hybrid Plastics (Fig. 1). Octaisooctyl-POSS is constituted by mixture of eight, ten and twelve silicon atoms cages. PP was a Moplen HP501L (MFR 6.0 g/10 min at 230 °C/2.16 kg) from Basell.

Composites were prepared mixing PP and POSS in a Brabender internal mixer W50E (180 °C, 10 min, 60 rpm). POSS was loaded into the polymeric matrix at different weight ratios, from 3 to 10 wt%.

The obtainment of PP/ome and oib-POSS nanocomposites was reported through the use of a twin screw extruder [28]. Nevertheless in this research we approached the preparation of PP/POSS composites by the use of a Brabender internal mixer. This choice was done on the basis of our experience on polymer/layered silicates nanocomposites; such experiences have been recently confirmed by others [29]. In the cited work, intercalated PP/clay composites were obtained indifferently through the use of a co-rotating twin screw extruder and of an internal mixer.

Moreover the brabender mixer allowed us to increase the residence time, thus extending the mechanical action effect.

X-ray (WAXD) diffraction patterns were obtained on a ARL XTRA48 diffractometer using Cu K_α radiation ($\lambda =$ 154,062 Å).

Scanning electron microscopy imaging was obtained by means of a LEO 1450 VP instrument; two different sample typologies were examined: either room temperature or cryogenic fracture surfaces (on samples cooled in liquid nitrogen).

Transmission electron microscopy (TEM) analysis was kindly supplied by the Department of Chemistry and Industrial Chemistry of Genoa University. TEM measurements were performed with a high-resolution transmission electron microscope (JEOL 2010). Ultrathin sections of about 100 nm thick were cut with a Power TOMEX microtome equipped with a diamond knife and placed on a 200-mesh copper grid.

Differential scanning calorimetry (DSC) analyses were run using a TA Q1000 instrument in hermetic aluminium pans, under nitrogen flow (50 ml/min). Except when differently indicated, heating rate was 10 °C/min from 0 to 200 °C performing three successive runs (heating–cooling–heating), with ca. 4 mg samples.

Thermogravimetry (TGA) was performed on a TA Q 500 instrument, on ca. 10 mg samples, in platinum pans, with gas fluxes of 60 ml/min for sample gas (nitrogen or air), and 40 ml/min for balance protection gas (nitrogen) on heating at 10 °C/min, between 50 and 800 °C.

For comparison, analyses were also performed on pure PP treated in a Brabender mixer in the same condition used to prepare the composites.

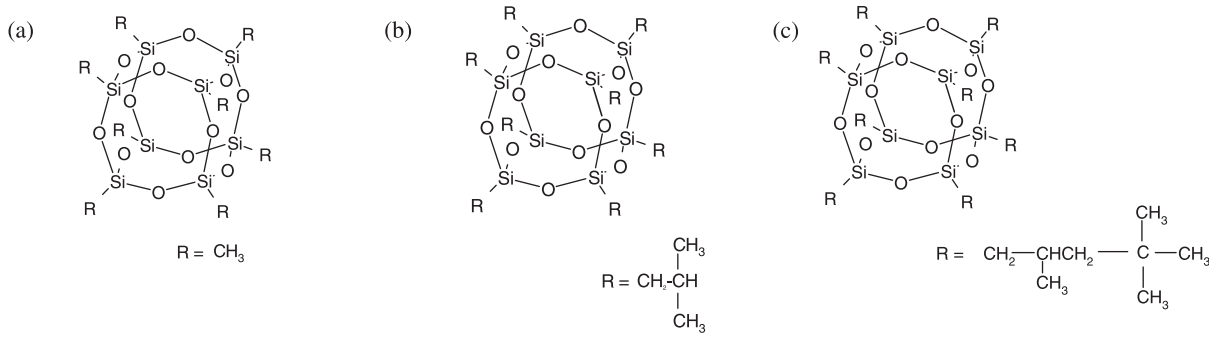

Fig. 1. (a) ome-, (b) oib-, (c) oic-POSS cage structures.

3. Results and discussion

3.1. Morphology

Morphological analyses were performed by means of SEM and XRD measurements.

3.1.1. PP–octamethyl-POSS

As evident from Fig. 2, a poor dispersion of the POSS within the polymeric matrix is achieved since micro aggregates (10–20 μm) of inorganics are found both at low and at high POSS loadings (Fig. 2(a) and (b), respectively).

This morphology also reflects on the XRD pattern of the 10 wt% loaded sample, reported in Fig. 3, in which the spectra of neat PP, of as-received ome-POSS and of the composite are compared. The POSS is highly crystalline, showing a very intense main diffraction peak at 2θ 10.5°. It is apparent that the trace from the composite shows crystalline features characteristic of both *i*-PP and POSS, confirming the presence of large POSS crystalline aggregates, as already found by SEM analysis.

We can presume that the extent of aggregation between the POSS cages is dominant on the chemical compatibility with the polymeric matrix given by the methyl substituent groups. Therefore, we could only achieve the distribution allowed by the mechanical action inside the internal mixer.

3.1.2. PP–octaisobutyl-POSS

In Fig. 4 are compared the fracture surfaces of neat PP and of 3 wt% oib-POSS loaded sample: in the former no specific morphological features can be detected while the latter shows fracture lines converging in a single point indicating a spherulite morphology of the PP crystals (highlighted in Fig. 4(b)). No POSS aggregates are visible by means of SEM analysis but TEM micrographs (Fig. 6(a)) clearly indicate the presence of POSS regular crystals with average dimensions of ca. 500 nm.

We suggest that the impossibility to single out POSS crystals in SEM micrographs may be due to an extremely good adhesion of the POSS crystals to the polymeric matrix so that the low temperature fracture does not find the interfaces POSS/PP as weak points to propagate through.

This spherulitic morphology is more evident when POSS loading is increased. By means of SEM analysis on two types of fracture surfaces of a 10% oib-POSS–PP composite we could understand the morphological characteristics of the PP composite and the role that POSS plays in determining this morphology. When a room temperature fracture is performed, the surface is constituted by PP spherulite surfaces (Fig. 5(a)): the fracture proceeds in the interspherulite region so that well defined and regular spherulite boundaries are visible.

Differently, when a low temperature fracture is performed, it proceeds in the intraspherulite region and the nature of the single spherulite is shown (Fig. 5(b)).

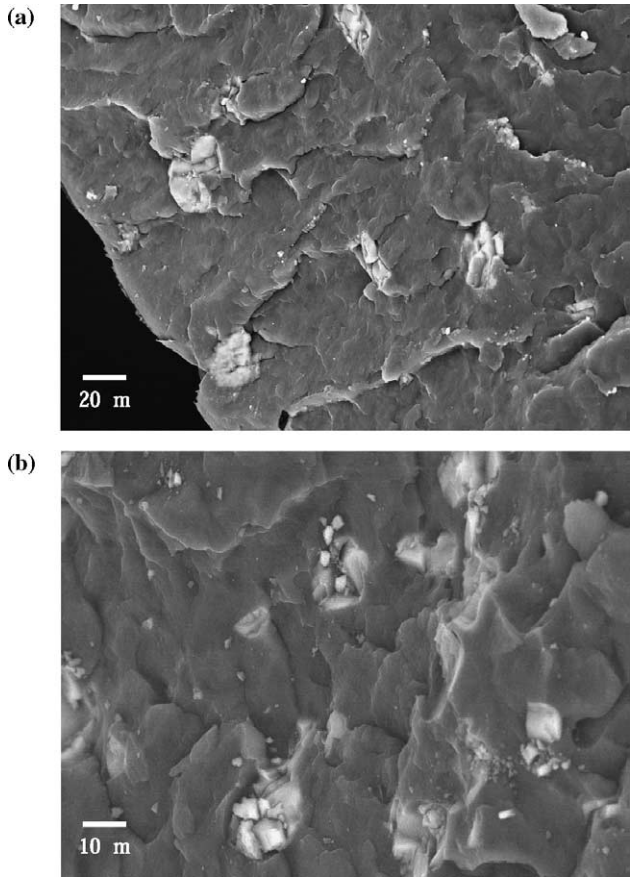

Fig. 2. PP/ome-POSS SEM micrographs; (a) 3%, (b) 10% POSS content.

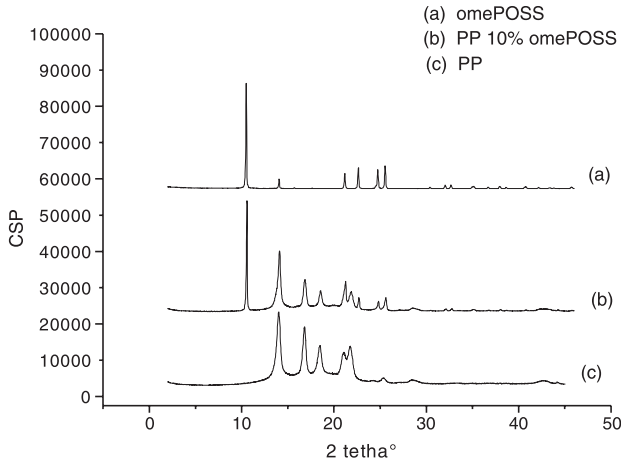

Fig. 3. XRD diffrattograms of as-received ome-POSS ((a) out of scale), neat PP (c) and 10 wt% composite (b). Curves have been shifted for clarity.

A regular POSS aggregate is found in the centre of each spherulite, acting as a sort of nucleating agent. In this case, the higher dimensions of the POSS aggregates can give reasons for the lower adhesion of the inorganic to the polymeric matrix, the interactions among POSS molecules being stronger than those between POSS and PP, thus generating fragile interfaces.

POSS crystals are also visible by means of TEM analysis

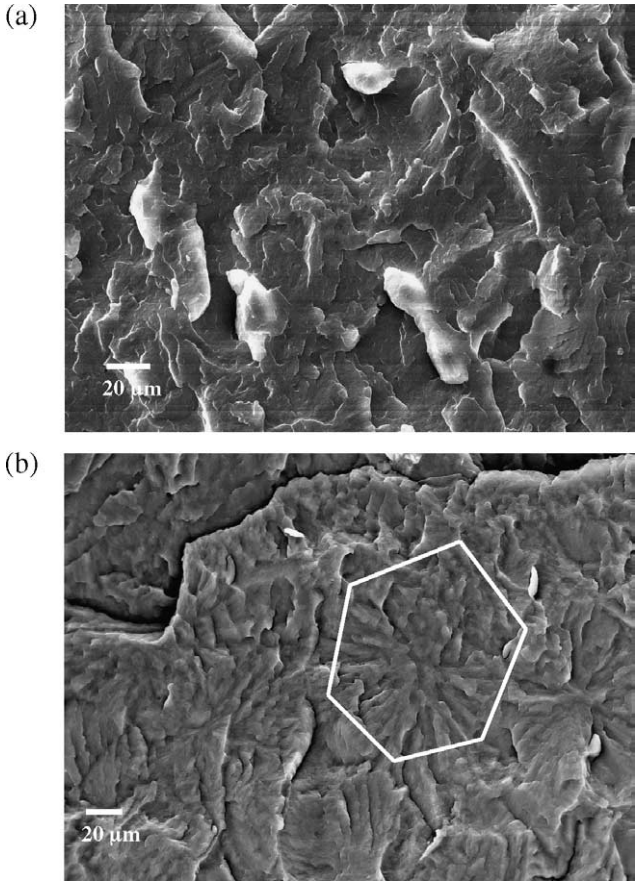

Fig. 4. SEM micrographs: (a) PP; (b) PP/3% oib-POSS.

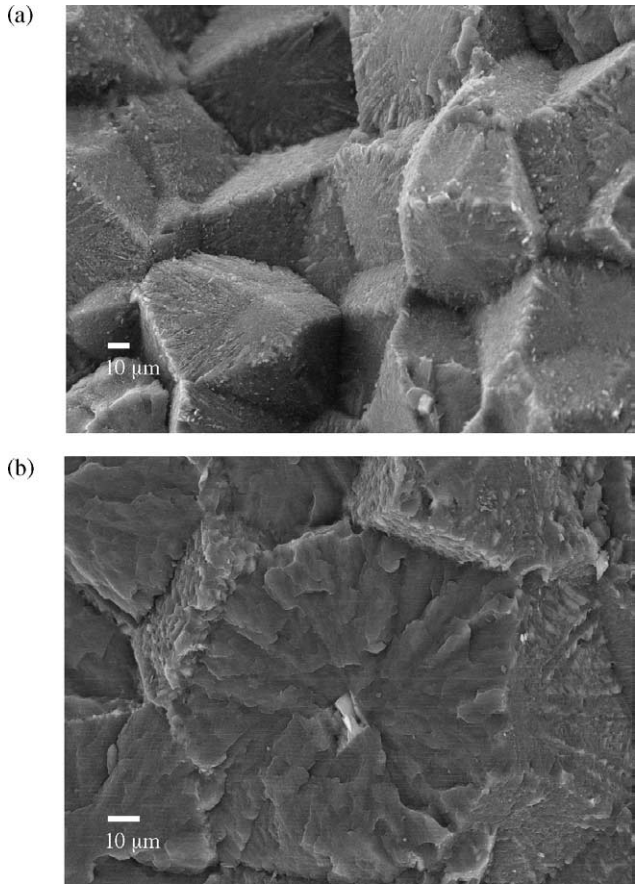

Fig. 5. PP/10% oib-POSS: (a) Room temperature fracture; (b) low temperature fracture.

(Fig. 6(b)); the arrangement in a preferential direction suggests the presence of POSS at spherulite boundaries.

In this case, the presence of POSS aggregates at grain boundaries could explain the morphology observed after room temperature fracture, characterising these regions with a scarce adhesion between the components, thus promoting the propagation of the fracture.

In any case the POSS crystals observed by means of TEM imaging inside the composite have different features if compared with the neat POSS crystals since they are characterised by high regular shape and bigger dimensions.

XRD analysis on the above samples indicates that the presence of oib-POSS within the polymeric matrix not only affects the morphology of the resulting composites, but also the way in which PP crystallises.

In Fig. 7 are reported the XRD patterns of neat PP, as-received oib-POSS and of the composites at different oib-POSS loadings.

As in the case of ome-POSS, we are analysing a highly crystalline specimen with two major intensity diffraction peaks at 2θ 8 and 8.8° (curve d) [30].

At low POSS loadings (curve b) the XRD spectrum shows crystalline features only referable to the PP matrix (curve a). However, we know from TEM analysis that POSS

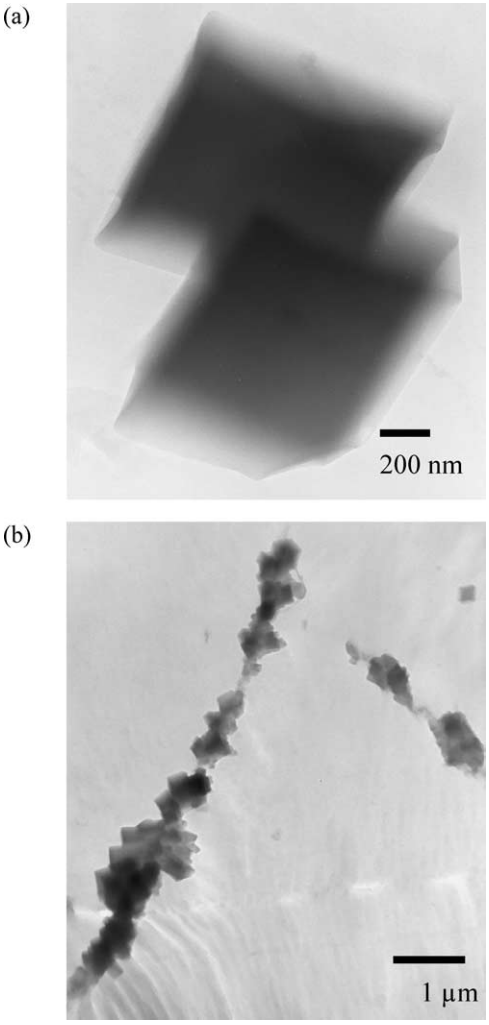

Fig. 6. PP/oib-POSS TEM micrographs: (a) 3 wt%; (b) 10 wt%.

crystallites are present in the polymeric matrix (Fig. 6(a)). In this respect, a significant role is likely to be played by the low concentration and by the extent of dispersion of fine aggregates that could hinder their detection by means of XRD analysis.

When increasing POSS concentration (curve c) diffraction patterns referable to the POSS crystalline structure are visible; we can notice in fact the appearance of the main diffraction peaks of the inorganic filler at $2\theta < 10°$. This is in complete accordance with what already observed by means of TEM analysis for the 10 wt% loaded sample (Fig. 6(b)).

Moreover, new features are present in the diffraction region of the PP matrix as new signals appear at 2θ 16 and 19.8°, as shown in the insert of Fig. 7, which are probably due to PP polymorphism.

In the crystalline state, it has been long recognised that PP exist in several different primary crystalline forms (α, β, γ) [31,32], the dominating one being the α-form. These forms exhibit different crystallographic symmetries and/or ordering of the isotactic chains.

As far as XRD analysis is concerned, the α-form is characterised by a strong diffraction peak at 2θ 18.6° [33], the β-form at 2θ 16.2° [32], and the γ-form at 20.1° [34].

We assume that the diffraction peaks at 2θ 16.0 and 19.8° appearing in the presence of oib-POSS in spectra of Fig. 7(b) and (c) can be attributed PP β and γ-forms, respectively. Slight shifts from the literature values are observed for the three phases.

3.1.3. PP–octaisooctyl-POSS

Analysing the morphology of the prepared composites by SEM imaging (Fig. 8). POSS aggregates could not be detected, neither in the 3 wt% nor in the 10 wt% composite; moreover, a spherulitic morphology could be appreciated in

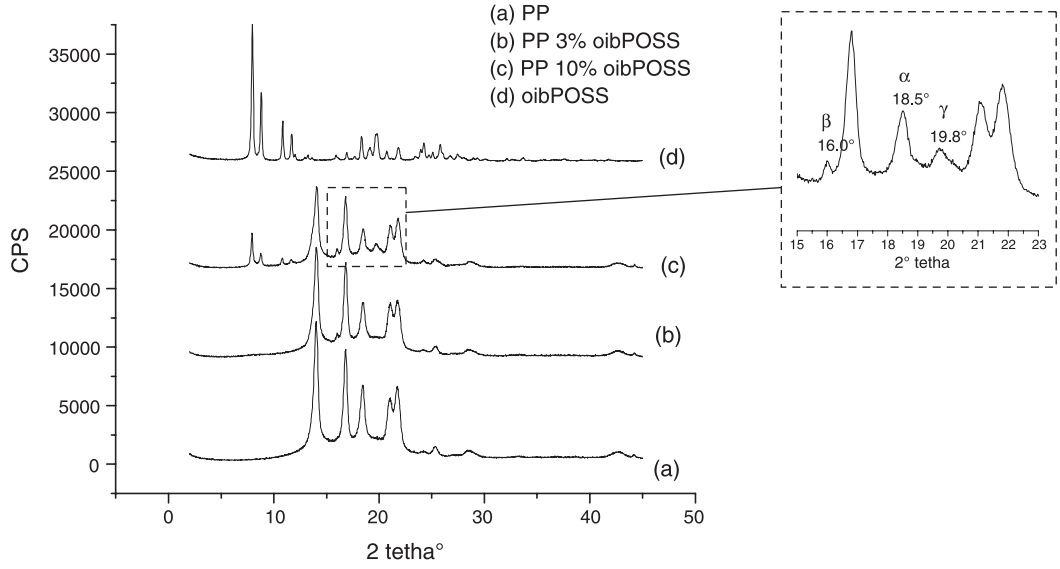

Fig. 7. XRD diffrattograms of as-received oib-POSS ((d) out of scale), neat PP (a) and 3 (b) and 10 (c) wt% composites. Curves have been shifted for clarity.

the 10% sample only analysing the interior of holes found within the polymeric matrix (Fig. 8(b)).

It must be noticed that oic-POSS is a liquid so that one would expect, rather than the aggregates of solid POSS observed in the previous micrographs, some liquid POSS domains.

No TEM analysis could be performed on these samples because thin sections of good quality could not be obtained since big tears were formed during sample slicing. This behaviour could be due to the presence of big POSS domains, within the PP matrix, characterized by a poor interface adhesion with the matrix itself.

XRD analysis in this case is little helpful in determining the morphological characteristics of the composites (Fig. 9) because the as-received POSS (curve a) being a liquid is characterized by an amorphous halo at 2θ ca. 7°. The halo, even though with a very low intensity, is visible in the 10% sample (curve d), suggesting the presence of POSS domains in the polymeric matrix. The low intensity of the POSS signal in the 10% composite is likely to be due, in addition to dilution, to the amorphous nature of oic-POSS that generates a low intensity signal also in the XRD pattern of neat POSS.

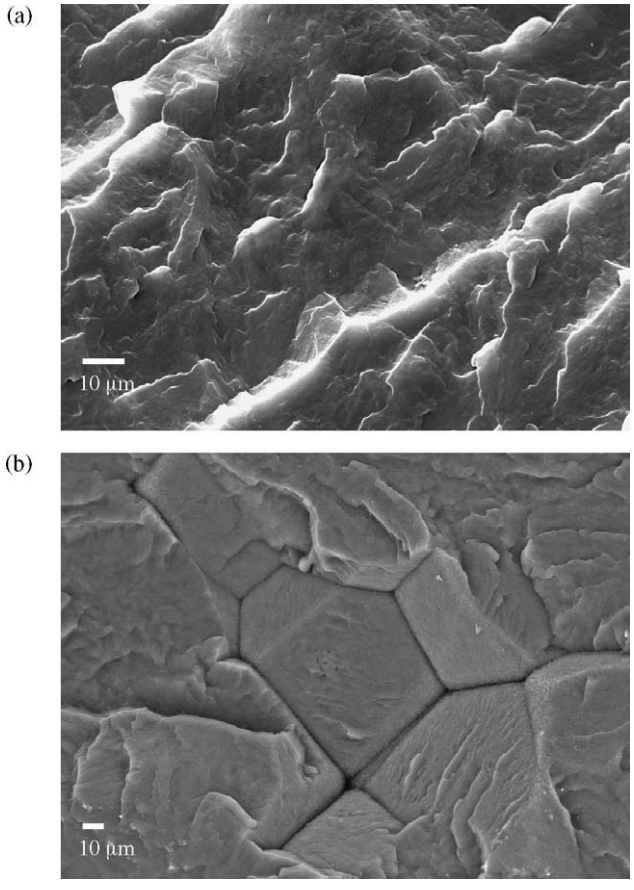

Fig. 8. PP/oic-POSS SEM micrographs; (a) 3%, ((b) hole, internal surface) 10% POSS content.

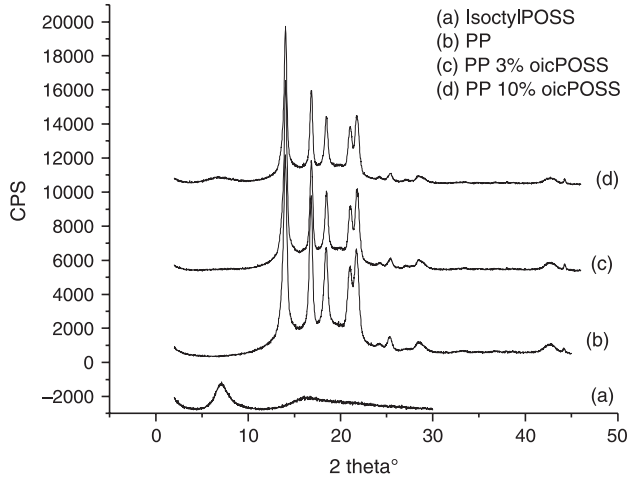

Fig. 9. XRD diffrattograms of as-received oic-POSS (a), neat PP (b) and 3 (c), 10 wt% (d) composites. Curves have been shifted for clarity.

3.2. Thermal behaviour: differential scanning calorimetry

The influence of the presence of the POSS on the crystallisation and melting behaviour of the PP matrix was evaluated by means of DSC analysis.

3.2.1. PP–octamethyl-POSS

No significant differences are brought by the presence of POSS in the melting temperature in comparison with pure PP; on the other end, as evident from Fig. 10, the crystallisation temperature is slightly increased: From 114 °C in neat PP to ca. 116 °C in the composites.

In Table 1 are reported the significant data as determined from the above DSC curve; T_o being the onset temperature, T_p the exothermic peak temperature and T_e the end temperature of crystallisation. It is evident that the presence of ome-POSS influences the crystallisation behaviour of the matrix as the crystallisation temperature is increased, both at 3 and at 10 wt%, by 2–3 °C.

As already stated by Fu et al. [25] for PP, high loadings

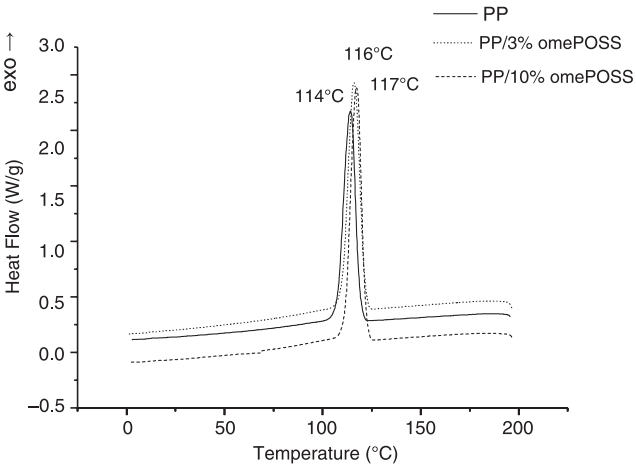

Fig. 10. DSC cooling curves of PP and ome-POSS containing composites.

Table 1
Nonisothermal crystallisation parameters for PP and PP/ome-POSS composites

Crystallisation parameters	PP (°C)	PP 3% ome-POSS (°C)	PP 10% ome-POSS (°C)
T_o	123	125	125
T_p	114	116	117
T_e	102	106	106

of ome-POSS (from 10 to 30 wt%) have a nucleating effect on the PP matrix as the degree of supercooling required for crystallisation is reduced in the presence of POSS, thus increasing the crystallisation temperature.

The same nucleating effect was found for HDPE by Joshi et al. [27]. In this last case, the nucleation effect (considering the exothermic peak maximum) was claimed taking into account differences in the order of 0.3–0.4 °C and was observed only for 10 wt% loadings.

Differently from what stated by the above mentioned research groups, we can observe a nucleating effect even at lower POSS content with 2–3 °C of difference in T_p.

This phenomenon has been recently studied for another class of nanofillers: organomodified montmorillonite was shown to influence the nonisothermal crystallisation of PP-*grafted*-maleic anhydride increasing the crystallisation rate, the activation energy and the nucleation activity [35,36].

3.2.2. PP–octaisobutyl-POSS

At variance with ome-POSS, DSC does not underline any significant feature concerning the behaviour during crystallisation of PP.

Conversely, differences are encountered in the behaviour of the composite at melting; in fact, a significant decrease in the melting temperature of PP is found, likely due to PP polymorphism, already identified by means of XRD analysis (Fig. 7): both β and γ forms, indeed, are known to have equilibrium melting temperatures lower than that of the α phase that is predominant in pure PP [37] (Fig. 11).

3.2.3. PP–octaisoctyl-POSS

As far as regards the crystallisation behaviour of the composites, the same conclusions, already seen for the oib-POSS composites, can be drawn also for oic-POSS.

Also, similarities are encountered in the melting behaviour as the melting peaks of the composites are shifted to lower temperatures (Fig. 12) but, while in the case of oib-POSS this could be attributed to polymorphic features, in this case the XRD pattern does not acknowledge for any other PP phase different from the α one (Fig. 9).

3.3. Thermal behaviour: thermogravimetric analysis

The influence of the presence of the POSS on the thermal behaviour of the PP matrix was evaluated by means of TGA analyses.

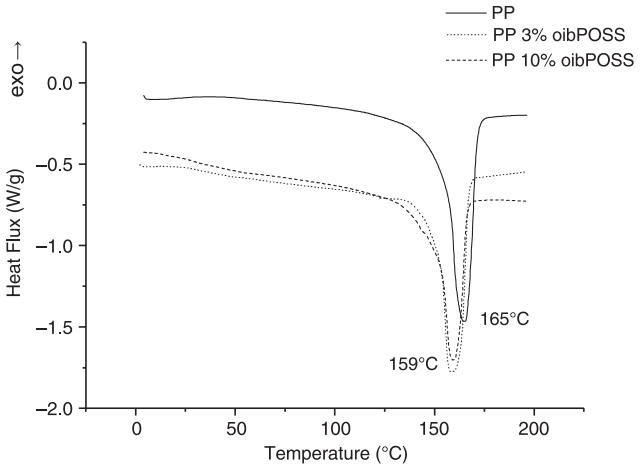

Fig. 11. DSC second heating of PP and PP/oib-POSS composites.

3.3.1. PP–octamethyl-POSS

TGA in nitrogen of PP–ome-POSS compounds (Fig. 13) reveals a complete coincidence between the composite and the PP matrix degradation path ($T > 400$ °C) as regards both the maximum weight loss rate temperature ($T_{max} = 460$ °C) and the residue amount at 750 °C. The presence of POSS does not affect the degradation mechanism of PP. A significant feature can be identified in the 10 wt% ome-POSS composite degradation path below 400 °C, in which ome-POSS should volatilise with maximum rate at 261 °C, as shown by the curve in Fig. 13, in comparison with the one calculated by linear combination of PP and ome-POSS thermogravimetric curves. Indeed ome-POSS in the composite shows a maximum volatilisation rate at 317 °C, probably due to POSS entrapment in the polymeric matrix.

The fact that PP in the composite degrades with a maximum rate temperature totally coincident with that of neat PP can be explained considering that, when the suitable temperature for the degradation of the matrix is reached, a negligible amount of ome-POSS is present in the composite, due to its lower volatilisation temperature.

A different composite behaviour is found in the

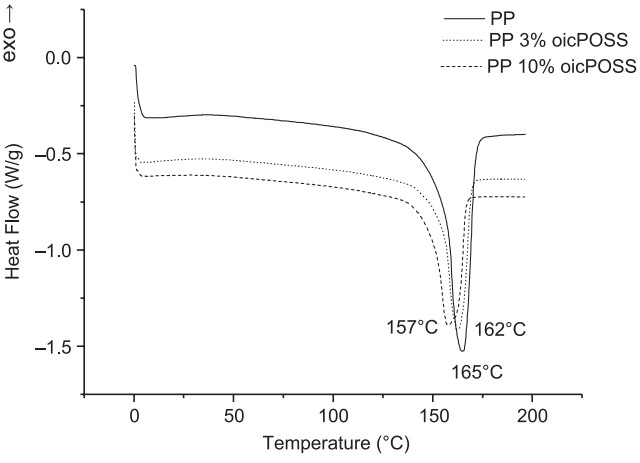

Fig. 12. DSC second heating of PP and PP/oic-POSS composites.

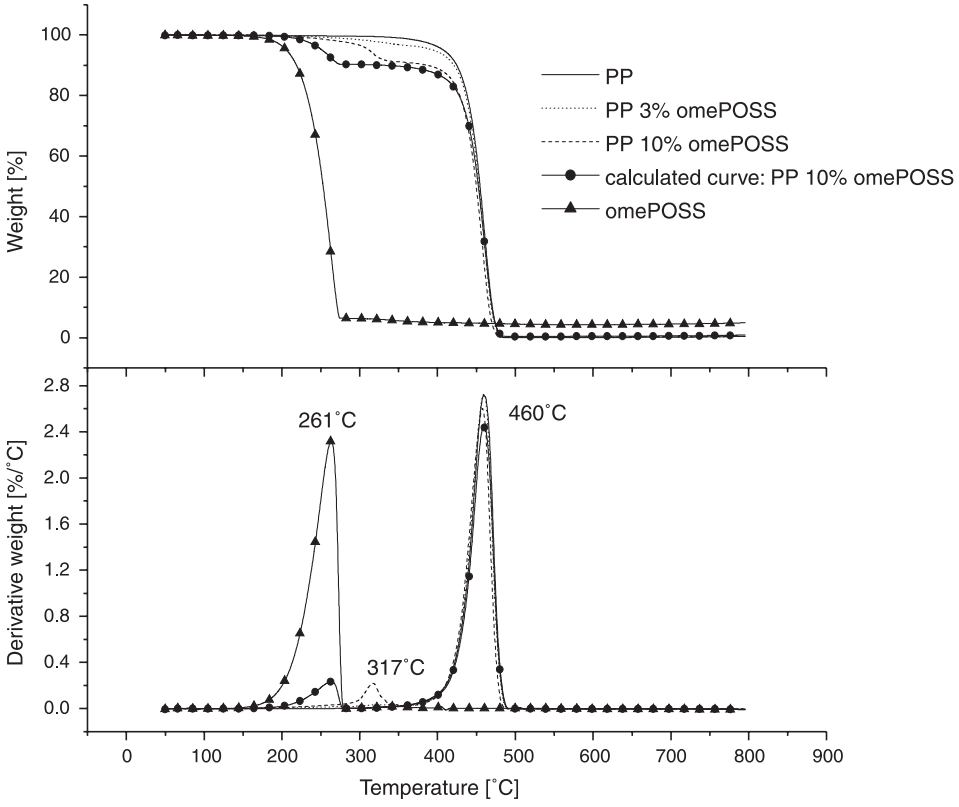

Fig. 13. TGA and DTA curves in nitrogen of PP and ome-POSS containing composites.

thermoxidative degradation in which the temperature of PP volatilisation is lowered by about 140 °C owing to the simultaneous effect of heat and reaction with oxygen (Fig. 14). Indeed, even at the lowest loading (3%), the temperature of maximum rate of weight loss is up-shifted by 12 °C as compared to neat PP. By adding a 10 wt% of POSS a further increase in the peak temperature is found, but not as significant as at lower loadings.

When analysing the calculated curve, obtained by linear combination, as described above, one can easily understand the reason why in air, ome-POSS is able to influence the degradation path of PP. Neat ome-POSS does not undergo an oxidation process: the volatilisation observed in nitrogen (Fig. 13) still occurs in air (Fig. 14) at the same temperature and with the same amount of residue (ca. 4% at 600 °C). Therefore, when PP starts its degradation process, ome-POSS is still present in the composite, its evaporation being not yet completed; for this reason we assume that ome-POSS does play a protective action towards PP, likely forming a surface layer restricting diffusion of oxygen within the matrix.

Despite this stabilisation effect, also in this case no influence is found on the amount of residue, which is in any case negligible.

3.3.2. PP–octaisobutyl-POSS

TGA analysis performed in nitrogen does not reveal any effect of the PP–oib-POSS combination on the degradation path of the composite (Fig. 15). In particular, the volatilisation of oib-POSS takes place at the temperature (maximum rate at 265 °C) predicted by the thermogravimetry of pure oib-POSS, as shown in Fig. 15 by complete coincidence of calculated and experimental curve for 10% oib-POSS loading.

Again, reasons for the above described behaviour can be found in the fact that, at the temperature at which PP starts its degradation process, oib-POSS is almost completely evaporated, as can be seen by oib-POSS TGA and DTA curves reported in Fig. 15. In fact, we already reported that oib-POSS evaporates upon melting at 265 °C when heated alone in these working conditions [30].

When analysing the thermoxidative behaviour of the composites, a significant delay in the maximum weight loss rate temperature is found (Fig. 16): the PP degradation peak (T_{max} = 319 °C) is shifted to higher temperatures and slightly broadened while the onset temperature is maintained constant. This is due to the shielding effect towards oxygen, which is more significant as the weight ratio of POSS in the composite is increased. Indeed, the maximum weight loss rate temperature shifts from 320 °C of the calculated curve to 328 and 349 °C for the 3 and 10 wt% loaded samples, respectively.

Oib-POSS can build up the surface shield because, although the maximum rate of the major weight loss in air occurs at 261 °C as in nitrogen, the residual weight at 800 °C in air is no longer negligible (ca. 26%), but a significant

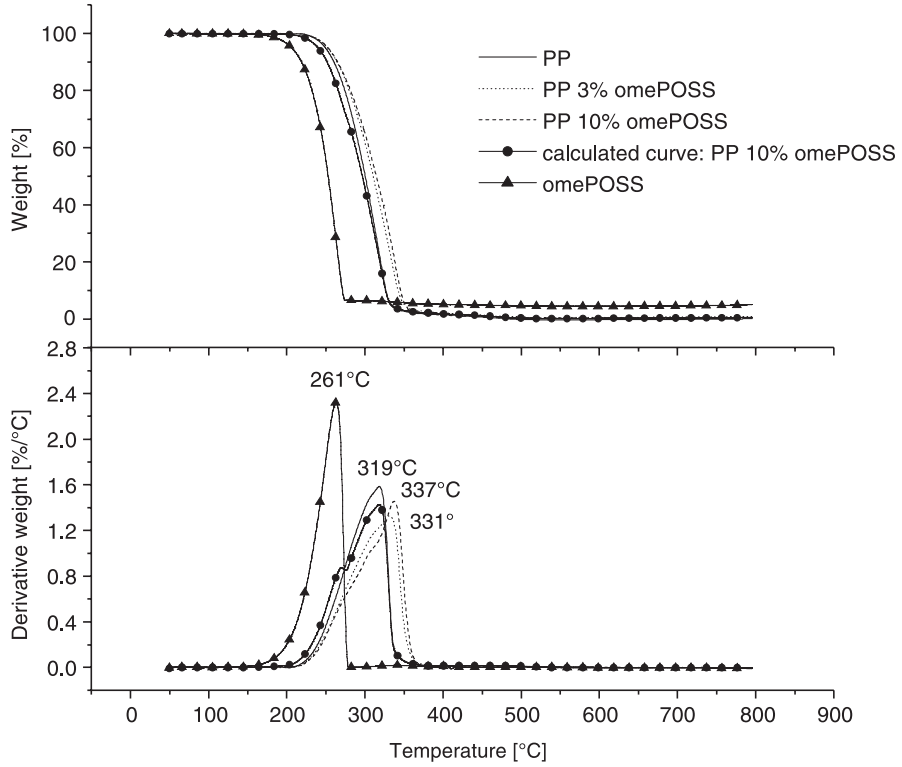

Fig. 14. TGA and DTA curves in air of PP and ome-POSS containing composites.

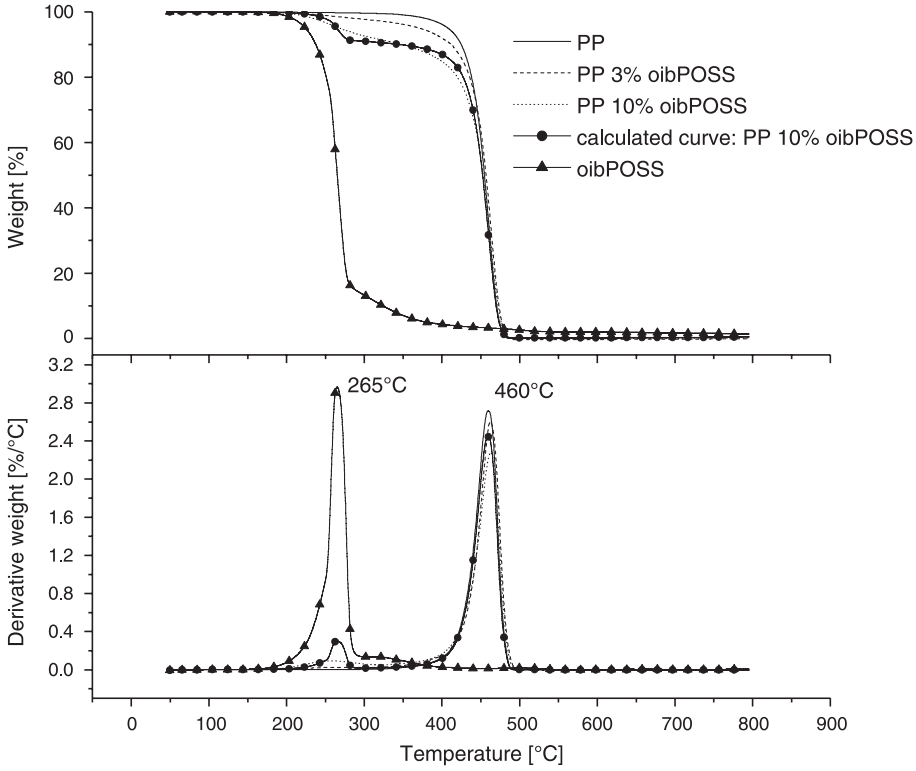

Fig. 15. TGA and DTA curves in nitrogen of PP and oib-POSS containing composites.

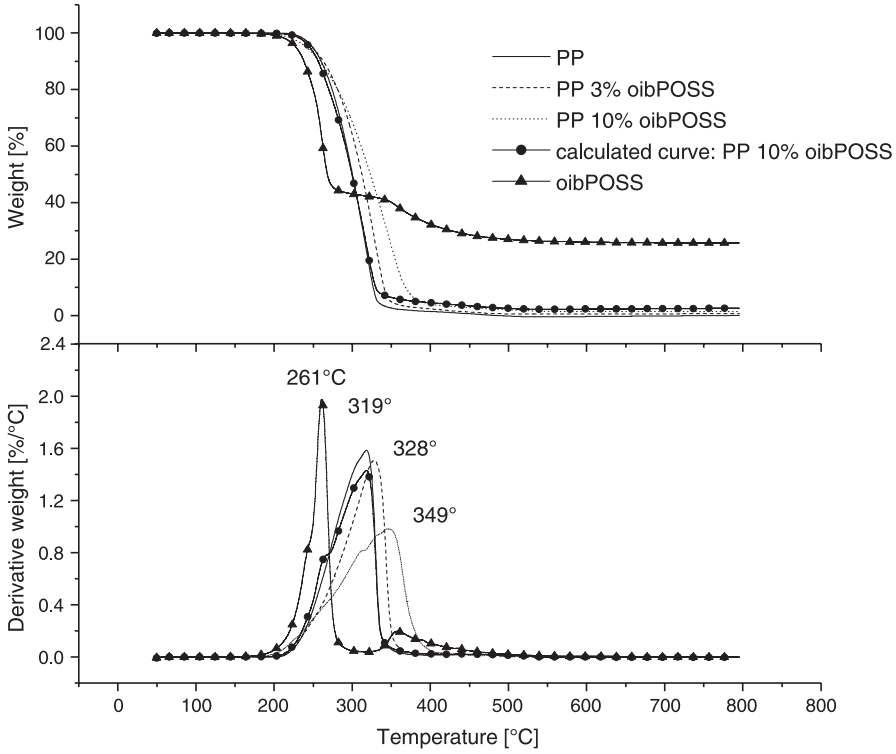

Fig. 16. TGA and DTA curves in air of PP and oib-POSS containing composites.

amount of thermally stable residue is found. Evaporation upon melting (that is typically found in inert atmosphere) is counterbalanced by the oxidation of oib-POSS. The residue left was found to have a silica-like structure by means of FT-IR analysis [30].

We can ascribe the different behaviour in air of ome-POSS and oib-POSS to the nature of the POSS cage substituents, since, while in methyl groups only inert primary protons are present, the isobutyl ones contain also more reactive tertiary protons. The latter, being more sensitive to the action of oxygen, promote the occurrence of oxidation reactions in competition with the evaporation process. This behaviour makes, therefore, possible the shielding effect by means of the silica formed by fast oxidation of the organic part of oib-POSS. The barrier towards oxygen does not imply the formation of a stable residue at the end of composite degradation process, rather a significant increase (ca. 12 °C) in the maximum weight loss rate temperature: 349 °C with oib-POSS vs. 337 °C with ome-POSS.

3.3.3. PP–octaisooctyl-POSS

In Fig. 17 are shown the degradation patterns of the composites in nitrogen: no significant changes are brought to the thermodegradative behaviour of neat PP but, differently from what previously reported in the case of high loaded oib-POSS and ome-POSS composites, at 10% loading no peak is detected referable to the volatilisation of the inorganic filler.

From the calculated curve we would expect a two step weight loss with the minor degradation signal at T_{max} = 375 °C, while only a small shoulder to the major weight loss peak can be seen at this temperature for the experimental curve. We can assume also in this case a behaviour similar to that already encountered for ome-POSS, i.e. a delay in the evaporation process due to entrapment in the polymeric matrix.

As regards the thermoxidative degradation process, we could notice a peculiar influence of the oic-POSS on the thermoxidative degradation of the polymeric matrix: the presence of a 3 wt% of oic-POSS increases the weight loss temperature from $T_{max,calc}$ = 319 °C of the calculated curve to T_{max} = 326 °C (Fig. 18) while at higher POSS loadings the experimental curve almost coincides with the calculated one.

The thermoxidative degradation process of oic-POSS is somewhat different from what previously encountered as it occurs in two steps (T_{max} 306 and 352 °C) both anticipated with respect to the maximum weight loss rate in nitrogen (372 °C); this multi step pattern could be due to the co-presence of POSS cages constituted by 10 and 12 silicon atoms. The complete characterisation of the degradation process will be the matter of further studies; nevertheless, we can already ascribe the stabilisation effect performed by oic-POSS towards PP to the formation of a stable residue after the two degradation steps (ca. 28% at 600 °C).

We can assume that a better extent of dispersion of the POSS at low loadings can allow for a better protection action.

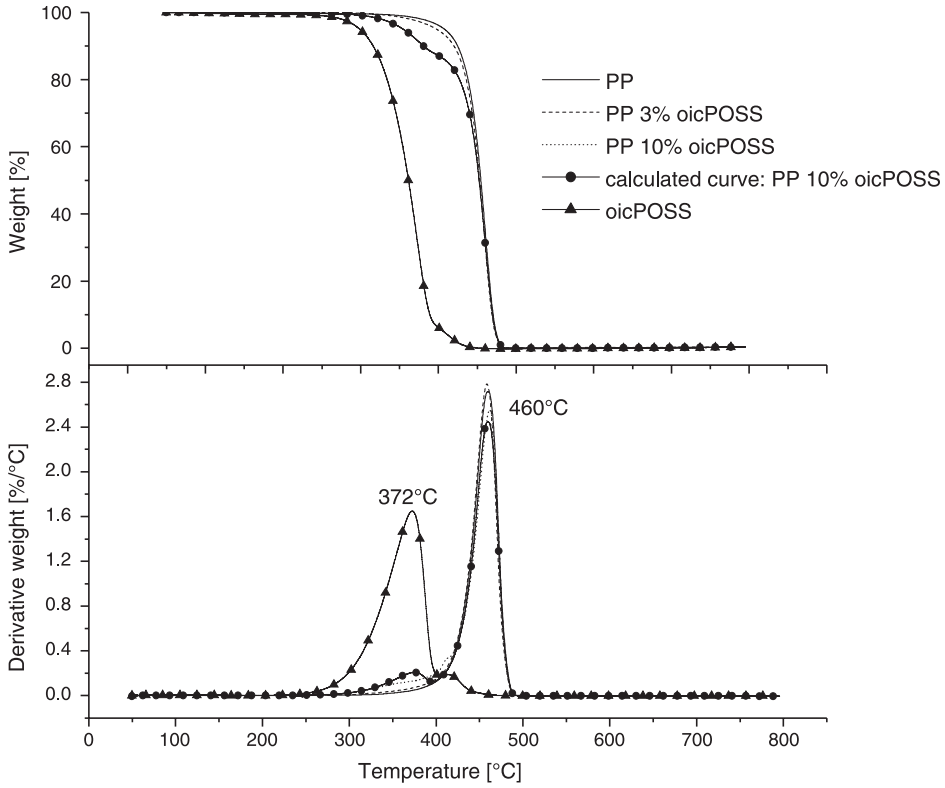

Fig. 17. TGA and DTA curves in nitrogen of PP and oic-POSS containing composites.

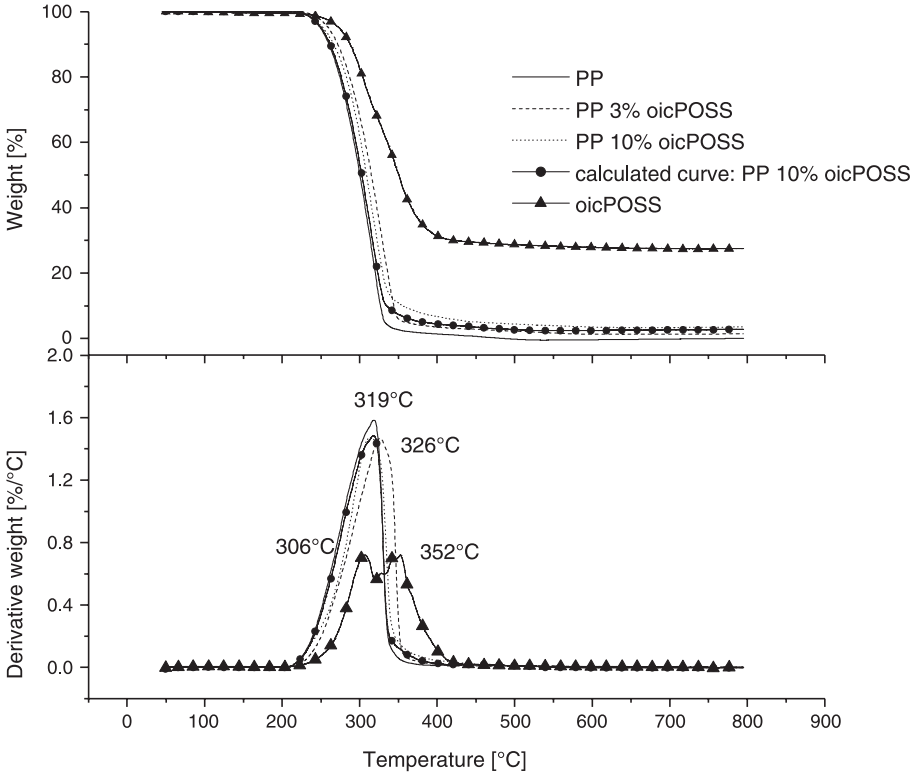

Fig. 18. TGA and DTA curves in air of PP and oic-POSS containing composites.

4. Conclusions

In this paper, the influence of POSS functionalisation on PP-based composites has been studied evaluating the effect of the different alkyl substituents on the thermal and morphological characteristics of the prepared composites.

Substantial differences have been found in the morphology of the composites by increasing alkyl chain length from octamethyl-POSS to octaisobutyl-POSS: in the first case, the compatibility between POSS and PP is very low and the filler is distributed within the matrix only by means of the mechanical action. On the other end, the *i*-butyl substituents are able to grant for a higher extent of dispersion, as determined by SEM imaging.

Further increase in the substituent chain length to isooctyl does not bring any apparent improvement on POSS dispersion although the liquid nature of oic-POSS makes SEM observation less diagnostic than in the cases of crystalline POSS.

Ome-POSS is found to act as a nucleating agent for PP, the crystallisation temperature being increased by 2–3 °C depending on the POSS content.

On the other end, oib-POSS is found to enhance the spherulitic morphology of PP acting probably as a growth centre and, moreover, to induce polymorphism in the matrix allowing for the crystallisation of the β and γ phases in addition to the more common α one.

The thermoxidative behaviour of the PP matrix is improved when adding the above fillers as an increase in the weight loss peak temperature is found at high POSS loadings. The effect which is more evident at higher dispersion extents (oib-POSS based composites) is due to oxygen scavenging by the inorganic phases cumulating on the surface of the material by polymer ablation.

Interesting features have emerged from this work, showing that the obtainment of nanocomposites with this class of inorganic filler as well as their characteristics are not simply driven by the length of the organic substituents, as one could predict on the basis of an expected increase in compatibility between the two phases. More complex, and worthy of further studies, interactions occur, leading to morphological and thermal characteristics whose origin is not yet completely understood.

Acknowledgements

This project was carried out in the frame of an Italian interuniversity research program (COFIN 2002) funded by the Ministry of Education, University and Research (MIUR). The authors would like to gratefully thank for TEM characterization Dr Orietta Monticelli of the Department of Chemistry and Industrial Chemistry in Genoa.

References

[1] Scott DW. J Am Chem Soc 1946;68:356.
[2] Li G, Wang L, Ni H, Pittman CU. J Inorg Organomet Polym 2001;11:123.
[3] Luecke S, Stoppek-Langner K. Appl Surf Sci 1999;144–145:713.
[4] POSS nanotechnology conference HB, CA; September 2002.
[5] Abbenhius HCL. Chem Eur J 2000;6:25.
[6] Lichtenan JD. Comments Inorg Chem 1995;17:115.
[7] Haddad TS, Lichtenan JD. Macromolecules 1996;29:7302.
[8] Romo-Uribe A, Mather PT, Haddad TS, Lichtenan JD. J Polym Sci, Part B: Polym Phys 1998;36:1857.
[9] Carrol JB, Waddon AJ, Nakade H, Rotello VM. Macromolecules 2003;36:6289.
[10] Sellinger A, Laine RM. Macromolecules 1996;29:2327.
[11] Costa ROR, Vasconcelos WL, Tamaki R, Laine RM. Macromolecules 2001;32:5398.
[12] Zhang W, Fu BX, Seo Y, Schrag E, Hsiao BS, Mather PT, et al. Macromolecules 2002;35:8029.
[13] Tegou E, Bellas V, Gogolides E, Argitis P. Microelectron Eng 2004;73–74:238.
[14] Tsuchida A, Bolln C, Sernetz FG, Frey H, Muelhaupt R. Macromolecules 1997;30:2818.
[15] Zheng L, Farris RJ, Coughlin EB. Macromolecules 2001;34:8034.
[16] Zheng L, Waddon AJ, Farris RJ, Coughlin EB. Macromolecules 2002;35:2375.
[17] Waddon AJ, Zheng L, Farris RJ, Coughlin EB. Nano Lett 2002;2:1149.
[18] Lee A, Lichtenan JD. Macromolecules 1998;31:4970.
[19] Li GZ, Wang L, Toghiani H, Daulton TL, Koyama K, Pittmann CH. Macromolecules 2001;34:8686.
[20] Ramirez C, Abad MJ, Barral L, Cano J, Diez FJ, Lopez J, et al. J Therm Anal Calorim 2003;72:421.
[21] Abad MJ, Barral L, Fasce DP, Williams RJ. Macromolecules 2003;36:3128.
[22] Fu BX, Namami M, Lee A. Polymer 2003;44:7739.
[23] Usuki A, Kato M, Okada A, Kurauchu T. J Appl Polym Sci 1997;63.
[24] Kawasumi M, Hasegawa N, Kato M, Usuki A, Okada A. Macromolecules 1997;30:6333.
[25] Fu BX, Yang L, Somani RH, Zong SX, Hsiao BS, Phillips S, et al. J Polym Sci, Part B: Polym Phys 2001;39:2727.
[26] Fu BX, Gelfer MY, Hsiao BS, Phillips S, Viers B, Blansky R, et al. Polymer 2003;44:1499.
[27] Joshi M, Butola BS. Polymer 2004;45:4953.
[28] Lichtenan JD, Schwab JJ, Lee A, Phillips S. World Patent WO 01/27885; 2001.
[29] Lertwimolnun W, Vergnes B. Polymer 2005;46:3462.
[30] Fina A, Tabuani D, Frache A, Boccaleri E, Camino G. Fire retardancy of polymers: New applications of mineral fillers. Cambridge, UK: Royal Society of Chemistry; 2005.
[31] Miller RL. Polymer 1960;1:135.
[32] Turner-Jones A, Aizlewood JM, Beckett DR. Makromol Chem 1964;75:134.
[33] Natta G, Corradini P. Cimento Suppl 1960;15:40.
[34] Brueckner S, Meille SV. Nature 1989;340:455.
[35] Fornes TD, Paul DR. Polymer 2003;44:3945.
[36] Li J, Zhou C, Gang W. Polym Test 2003;22:217.
[37] Phillips RA, Wolkowicz MD. Polypropilene handbook. Munich: Hanser Publishers; 1996.